PHOTONICS Research

High-power wavelength-tunable and power-ratio-controllable dual-wavelength operation at 1319 nm and 1338 nm in a Q-switched Nd:YAG laser

Qi Bian,[1,2,3] Yong Bo,[1,2,3,4] Jun-Wei Zuo,[1,2,3] Lei Yuan,[1,2,3] Hong-Wei Gao,[1,2,3] and Qin-Jun Peng[1,2,3,5]

[1]Key Laboratory of Solid State Laser, Technical Institute of Physics and Chemistry, Chinese Academy of Sciences, Beijing 100190, China
[2]Key Laboratory of Functional Crystal and Laser Technology, Technical Institute of Physics and Chemistry, Chinese Academy of Sciences, Beijing 100190, China
[3]Institute of Optical Physics and Engineering Technology, Qilu Zhongke, Jinan 250000, China
[4]e-mail: boyong@tsinghua.org.cn
[5]e-mail: pengqinjun@mail.ipc.ac.cn

Received 20 May 2022; revised 10 July 2022; accepted 17 July 2022; posted 19 July 2022 (Doc. ID 462168); published 14 September 2022

We report the first demonstration on three types of 1.3 μm spectral region in a *Q*-switched Nd:YAG laser. In order to dissipate the heat deposition effectively to obtain good beam quality, the Nd:YAG rod crystal with 1° cut-angle on end faces is side-pumped by the quasi-continuous-wave pulsed laser diode. A Suprasil etalon is well designed as the intracavity mode-selector to obtain wavelength-tunable single line or power-ratio-controllable dual line operation at 1319 nm and 1338 nm. With the pump pulse width of 200 μs and pump power of 410 W, the acousto-optic *Q*-switched laser delivered a pulse width of 117 ns at 400 Hz repetition rate, and the M^2 factor was measured to be about 1.87. 1319 nm together with 1338 nm single-wavelength laser achieved an average output power of 47.6 W and 39.9 W with a linewidth of 0.48 nm and 0.32 nm, and a tunable range of 111.2 pm and 108.6 pm, respectively. Among dual-wavelength oscillation, both lines can be tuned at almost equal intensity level with 45.7 W total output power, which is input into an LBO crystal to generate red light of 11.4 W for 659 nm, 6.7 W for 664 nm, and 7.5 W for 669 nm. The 1.3 μm wavelength-selectable operation realized by using the same laser configuration may enhance the application in the fields of tunable lasers and THz frequency generation.

https://doi.org/10.1364/PRJ.462168

1. INTRODUCTION

High-power lasers in the 1.3 μm spectral region have attracted a surge of attention for their immense applications in remote sensing, surgery, military field, optical fiber communication, information storage, and so on [1–3]. By frequency doubling and frequency tripling, red and blue light can be further obtained with 1.3 μm laser emission, which has important applications in laser display and medical treatment [4,5]. Compared with continuous-wave operation, the *Q*-switching operation can provide high peak power with a narrow pulse duration in nanosecond scale. Therefore, the *Q*-switched lasers of 1.3 μm have been an interest of scientific research [6–9]. For instance, Wan *et al.* described a *Q*-switched 1319 nm laser from diode-side-pumped Nd:YAG crystal, and a maximum average power of 8.9 W of TEM_{00} mode was obtained at the repetition rate of 8 kHz [6]. Zhang *et al.* reported a high-power diode-side-pumped Nd:YAG laser emitting at 1338 nm, and the average output power at *Q*-switched operation decreased from 70 W at 50 kHz to 55 W at 5 kHz [7].

In addition, the simultaneous dual-wavelength laser at 1319 nm and 1338 nm has potential for the generation of ultrahigh repetition rate pulses by an optical beating, new-wavelength laser via sum-frequency and coherent terahertz (THz) radiation via difference frequency mixing [10,11]. However, the output power of dual-wavelength generation was at a relatively low level [12–15]. In 2010, a dual-wavelength operation Nd:YAG ceramic laser at 1319 nm and 1338 nm was demonstrated, which achieved the passively *Q*-switched average power of 226 mW with a pulse width of 15 ns at pulse repetition rate of 133 kHz [12]. Recently, a dual-wavelength passively *Q*-switched 1319 nm/1338 nm Nd:YAG laser by directly pumping at 885 nm was presented, and the maximum total output power was 3.55 W with a maximum repetition rate of 64.10 kHz [14].

In this paper, three types of high-power 1.3 μm Nd:YAG Q-switched lasers are successfully developed for the first time, operating at 1319 or 1338 nm single-wavelength, and power-ratio-controllable dual wavelength of 1319 and 1338 nm. These lasers, which are realized by means of optimizing the angle and temperature of the etalon in the cavity, deliver the output powers of 47.6 W for 1319 nm, 39.9 W for 1338 nm, and 45.7 W for balanceable dual-line oscillation. With the quasi-continuous-wave (QCW) pulsed laser diode (LD) pumping to mitigate the thermal effect in the crystal, the pulse width of a Q-switched laser is about 117 ns at a repetition rate of 400 Hz with a good beam quality of $M^2 = 1.87$. Furthermore, the red wavelengths of 659 nm, 664 nm, and 669 nm have been also studied by the frequency conversion technology with an LBO crystal. It is of important practical value that the versatile lasers at 1.3 μm could match the requirement of different applications.

2. EXPERIMENTAL SETUP

The Nd:YAG crystal is a very superior laser material because of the excellent thermal properties and laser characteristics [16]. In Nd^{3+} ions, there exist two strong overlapped stark transitions in the vicinity of 1.3 μm corresponding to ${}^4F_{3/2} \rightarrow {}^4I_{13/2}$, which are the R2–X1 transition irradiating 1318.8 nm wavelength and the R2–X3 transition irradiating 1338.2 nm wavelength. Their effective stimulated emission cross sections are as large as 8.7×10^{-20} cm^2 and 9.2×10^{-20} cm^2, respectively, which are only one-fifth of that of the R2–Y3 transition at 1064 nm. Because of the larger quantum defect and the stronger excited-state absorption, the thermal lens effect at 1.3 μm was stronger than that at 1.06 μm. Therefore, it is a challenge for 1319 nm and 1338 nm to obtain high-power coherent radiation at single wavelength or simultaneous dual wavelength.

It is essential to minimize the thermally induced negative impact on the stability of the laser cavity and laser efficiency. Here, the operation of a pulsed diode-pump is used for alleviating the thermal effects of the gain medium, which contributes to the generation of a more energetic pulse with good beam quality. The schematic of a 1.3 μm Nd:YAG Q-switched laser is shown in Fig. 1. Two laser modules LM1 and LM2 are homemade for power scalability, where a Nd:YAG rod of length 102 mm and diameter 3 mm with Nd^{3+} doping concentration of 0.6% was used as the gain medium. The central 72 mm of the rod was threefold symmetrically side-pumped by the QCW LD bars emitting at the wavelength of 808 nm, providing a maximum pump power of 360 W for the single laser module (LM) at 200 μs pulse width and 400 Hz repetition rate. A 90° quartz rotator (QR) was placed between the LMs to compensate the thermally induced birefringence. To obtain higher peak power, the Q-switched operation was realized using two fused silica acousto-optic modulators (AQs) driven at 27.2 MHz with a modulating signal in the range 100 Hz–50 kHz, which were placed orthogonally with each other to improve the hold-off capacity. Two concave lenses F1 and F2 are inserted into the cavity to enlarge the volume of the fundamental mode and filter out higher-order traverse modes, so as to obtain high output power with good beam quality. In order to suppress 1064 nm oscillation, the rear mirror M1 was coated with high reflection (HR) at 1.3 μm ($R > 99.8\%$) and high transmission (HT) at 1064 nm ($T > 95\%$), and the output coupler M2 was coated with a partial transmission at 1.3 μm ($T = 60\%$) and HT at 1064 nm ($T > 98\%$). The thin-film polarizer P1 was coated with HR at laser lines in the vertical direction and HT in the parallel direction at an incidence angle of 45°. The cavity length of the symmetric resonator was optimized to be 560 mm.

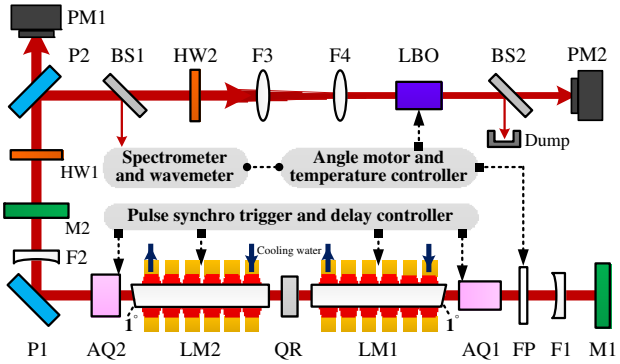

Fig. 1. Schematic diagram of the experimental setup for the 1.3 μm Nd:YAG Q-switched laser. M1, high reflector; M2, output coupler; P1, P2, thin-film polarizer; LM1, LM2, laser module; QR, 90° quartz rotator; AQ1, AQ2, acousto-optic Q-switch; F1–F4, lens; FP, Fabry–Perot etalon; HW1, HW2, half-wave plate; BS1, BS2, beam splitter; LBO, LiB_3O_5 crystal; PM1, PM2, powermeter.

Specifically, both end faces of the Nd:YAG rods were not only anti-reflection coated for 1064 nm and 1.3 μm, but also had a 1° cut-angle to ensure it has sufficient loss for 1064 nm strongest line to prevent lasing inside the two laser rods under high gain Q-switched mode. Moreover, a Fabry–Perot etalon FP is inserted into the cavity to achieve selectable wavelength oscillation by using the same laser. The angle of the etalon is precisely controlled by a piezo-driven tip/tilt platform, and its temperature is maintained by a temperature controller with a precision of ±0.05°C. In order to detect the wavelength of the output laser, the lasing beam was reflected into an optical spectrum analyzer by a beam splitter BS1. Based on the application requirements, the spectral purity of the single and dual wavelength at 1319 and 1338 nm could be chosen through the angle and temperature servo control of the etalon in a closed loop by a proportion-integration-differentiation (PID) module.

In order to examine the performance of 1.3 μm Q-switched laser, we carried out the nonlinear frequency conversion of the laser. An LBO crystal with cut of $\theta = 0°$ and $\varphi = 0°$ and a size of 4 mm × 4 mm × 30 mm was selected as the nonlinear material, which has the advantage of high conversion efficiency, high damage threshold, and no walk-off effect. The crystal is placed inside an oven and accurately manipulated by a temperature controller, by which type-II noncritical phase matching was realized. The combination of HWP1 and P2 was used to inject the output laser into powermeter PM1 or LBO crystal. HWP2 was used to adjust the polarization plane to fulfill the phase-matching condition. We employed two lenses F3 and F4 to reduce the beam diameter of the 1.3 μm laser with a ratio of

2:1 and reach proper input intensity, where the nonlinear conversion efficiency should be acceptable and the coatings should not be damaged. The collimated beam radius inside LBO was managed to be around 600 μm. A beam splitter BS2 was placed ahead of PM2 to separate the residual fundamental beam from the red beam.

3. RESULTS AND DISCUSSION

The pulse temporal characteristics of LD pumping and oscillating laser were recorded by a 1 GHz bandwidth digital oscilloscope (Tektronix DPO 4014B-L). Figure 2(a) shows the typical pulse trains of the LD pump and free running mode at a pulse repetition rate of 400 Hz. An extended single pulse profile of the free running laser is presented in Fig. 2(b) with the full width at half-maximum (FWHM) of 180 μs, indicating the laser building up time of ~20 μs. To realize high-energy pulse output, the time delay between the LD pumping and *Q*-switched modulator is set to be 200 μs. From the *Q*-switched pulse trains in Fig. 2(c), the peak-to-peak fluctuation is smaller than 6%, which can demonstrate the stable *Q*-switched operation. Figure 2(d) depicts an expanded single pulse profile of *Q*-switched operation with FWHM of about 117 ns.

Based on the theory of etalon [17], the thickness and reflectivity of the etalon should be optimized to make sure that the transmission curves of the 1319 nm and 1338 nm lines could be separated, so as to control the losses at the two lines. In the experiment, the etalon made of Suprasil 3002 (Heraeus) is designed to be 1 mm thick with the free-spectral range of 103 GHz and fineness of 1.1. Figure 3 depicts the transmission curves at 1319 nm and 1338 nm versus the tilt angle and temperature of the etalon. As shown in Fig. 3(a), maximum transmission difference between the 1319 nm and 1338 nm could be obtained by tuning the etalon to a proper tilt angle, where it will tend to oscillate at a single wavelength as a result of the mode competition, and the other one is restrained due to the higher insertion loss. On the other hand, simultaneous dual wavelength can occur at a certain value of transmission difference, and the intensity proportion varies with the transmission

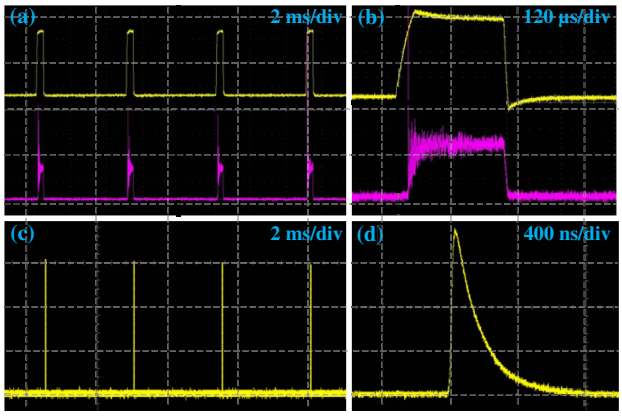

Fig. 2. Temporal profile of (a) the pulse trains for LD pump and free running mode, (b) enlarged single pumping pulse and free running laser pulse, (c) the pulse trains for *Q*-switched laser, and (d) enlarged single *Q*-switched laser pulse.

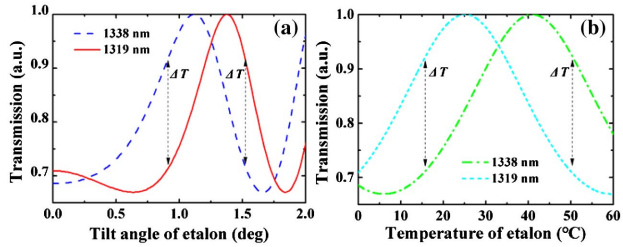

Fig. 3. Transmission curves at 1319 and 1338 nm versus (a) the tilt angle and (b) temperature of etalon with 1 mm thickness.

curves. It could be found from Fig. 3(b) that it is the same for the temperature tuning, which will be described below as a proof-of-concept demonstration.

The lasing spectra under different rotation angles of etalon are monitored with an optical spectrum meter (NIRQuest256-2.5 Ocean Optics Inc.), which is displayed in Fig. 4. When the etalon is maintained at an angle of 0.7 deg, one can see from Fig. 4(a) that only the single wavelength of 1338 nm was detected with a linewidth of about 0.32 nm. With rotating the angle to a certain value, the 1319 nm line began to oscillate, and the laser simultaneously operated at dual wavelength. At the beginning, the 1338 nm line was dominant, and the intensity proportion of the 1319 nm laser rose rapidly with the increase of the rotation angle. For example, the ratios between the intensities of 1319 nm and 1338 nm were near 1:2, 1:1, and 2:1 for the angle of 1.08 deg, 1.21 deg, and 1.3 deg, as shown in Figs. 4(b)–4(d). When the angle is increased to 1.5 deg, Fig. 4(e) shows that the laser operated at 1319 nm single wavelength with linewidth of about 0.48 nm. Consequently, three types of 1.3 μm *Q*-switched lasers were successfully developed, and the experimental result was well in agreement with the theoretical analysis.

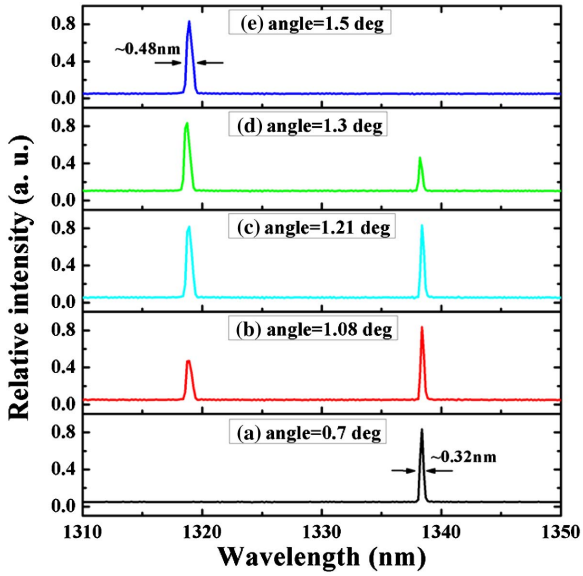

Fig. 4. Spectra with a wavelength range from 1300 nm to 1360 nm at different angle of etalon: (a) 0.7 deg, (b) 1.08 deg, (c) 1.21 deg, (d) 1.3 deg, and (e) 1.5 deg.

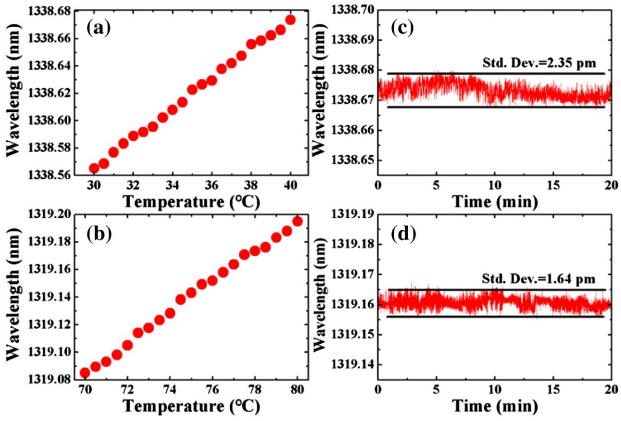

Fig. 5. Wavelength tuning of (a) 1319 nm and (b) 1338 nm versus the temperature of etalon, and stability measurement of (c) 1319 nm and (d) 1338 nm within 20 min.

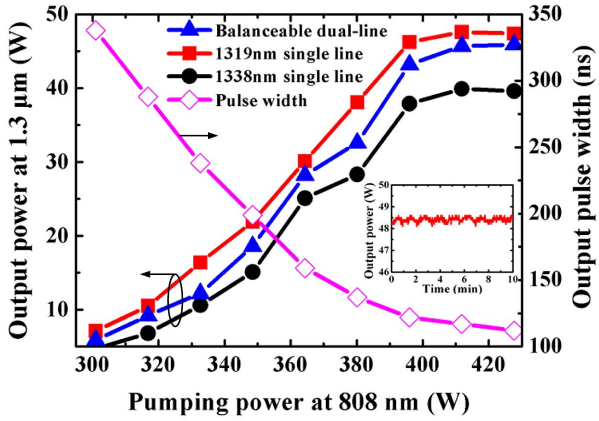

Fig. 6. Output power and pulse duration of 1.3 μm *Q*-switched laser as a function of incident pump power at 808 nm. Inset, power stability in 10 min.

Fine wavelength tuning and stability are critical issues for the single-wavelength operation, accomplished by adjusting the temperature of the etalon. At normal incidence, Fig. 5 shows the measured laser's wavelength with a wavelength meter (WS-7 HighFinesse GmbH). When the temperature was changed from 30°C to 40°C, the wavelength at 1338 nm was continuously tuned from 1338.5652 nm to 1338.6738 nm, as shown in Fig. 5(a), corresponding to a tunable range of 108.6 pm. For 1319 nm single line, a tunable range of 111.2 pm from 1319.0834 nm to 1319.1946 nm could be obtained with the increasing temperature from 70°C to 80°C, as shown in Fig. 5(b). The slope of both tuning curves was about 11 pm/°C, and the step-length of temperature was 0.05°C, which corresponds to wavelength tuning resolution of 0.55 pm. Meanwhile, there were no significant changes in the output power as the temperature of the etalon changes. Figures 5(c) and 5(d) show the stability measurement of output wavelength at 1338.673 nm and 1319.161 nm, where the standard deviations were less than 2.35 pm and 1.64 pm in 20 min, corresponding to a frequency stability of ±392 MHz and ±282 MHz, respectively.

Operating under single-wavelength and balanceable dual-wavelength oscillation of 1319 and 1338 nm, the dependence of the output power and pulse width on pumping power is plotted in Fig. 6. At a 400 Hz repetition rate, the output power of the 1.3 μm Nd:YAG laser grew gradually with the incident pump power from 300 W to 410 W, and the corresponding pulse width would be decreased from 338 ns to 117 ns. As the pump power increased to more than 410 W provided by two LMs, the output power exhibited roll-over behavior, which was presumably caused by the serious thermal lens effect that shifts the resonator's operation status away from the stable region and into the unstable zone. An analogous effect was also reported in previous publication [18]. As a result, 1319 nm together with 1338 nm single-wavelength laser achieved a maximum output power of 47.6 W and 39.9 W, respectively, corresponding to an optical-to-optical conversion efficiency of 11.6% and 9.7%. From the results, the highest peak power was numerically estimated to be as high as 1.02 MW with a pulse energy of 119 mJ at 1319 nm and 0.853 MW with a pulse energy of 99.75 mJ at 1338 nm. With simultaneous dual wavelength at 1319 nm and 1338 nm with intension ratio of 1:1, the measured average output power was 45.7 W with the optical conversion efficiency of 11.1%, corresponding to the peak power of 0.976 MW and single pulse energy of 114.25 mJ. The inset of Fig. 6 shows that the fluctuation at the maximum output power is measured to be better than 0.6% over 10 min, indicating the laser is a stable and reliable system, which is a prerequisite for practical applications. The beam quality recorded by a laser beam analyzer (CINOGY Technologies CS300-HP) is presented in Fig. 7. The beam quality factors are $M_x^2 = 1.76$ in the horizontal axis and $M_y^2 = 1.98$ in the vertical axis, which correspond to an average value of $M^2 = 1.87$. The inset in Fig. 7 exhibits a far-field two-dimensional (2D) beam intensity profile, which demonstrates that the laser operates at the fundamental transverse mode.

The output beam maintaining almost equal spectral contributions at 1319 nm and 1338 nm was employed as the fundamental pump source for the frequency conversion. The second harmonic generation (SHG) and sum-frequency generation (SFG) have been realized by manipulating the

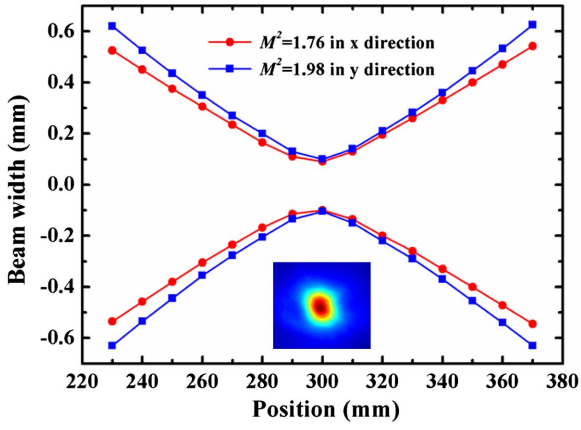

Fig. 7. Measured beam quality and far-field beam profile at the maximum output power.

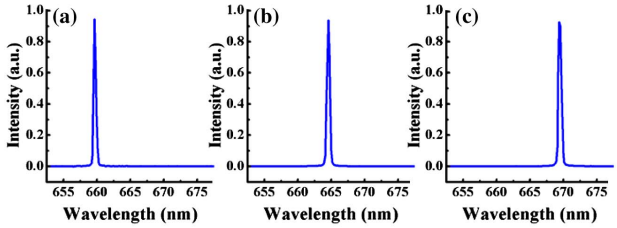

Fig. 8. Spectra of the red laser at (a) 659 nm for 45°C of LBO, (b) 664 nm for 42°C of LBO, and (c) 669 nm for 58°C of LBO.

phase-matched temperature of the LBO. The spectra of the visible lasers were measured by a spectrometer (AvaSpec-2048 FT-SPU), as illustrated in Fig. 8. When the temperature of LBO was set at 45°C, 42°C, and 58°C, red light with the wavelengths of 659.56 nm (SHG), 664.41 nm (SFG), and 669.29 nm (SHG) was detected without any other wavelength, respectively. The SHG and SFG output power as a function of the fundamental pump power was measured using a power-meter (OPHIR, FL400A-LP1-50), as described in Fig. 9. It is found that the red output power was almost linearly varying with the input fundamental pump power at 1.3 μm. At the highest input power of 46 W, we obtained 11.4 W at 659 nm, 6.7 W at 664 nm, and 7.5 W at 669 nm. The corresponding conversion efficiency was calculated to be 49.6% from 1319 nm to 659 nm, 14.6% from IR to 664 nm, and 32.6% from 1338 nm to 669 nm, respectively. And, it can be clearly found from Fig. 9 that they are not saturated, which suggests that there is a potential to obtain higher red power by means of increasing the input pump laser.

Figure 10 gives the measured power stability of the red 659 nm laser over 1 h. The mean power and standard deviation were 11.35 W and 0.088 W, corresponding to 0.8% relative deviation. The unstable laser power was attributed to the variation of fundamental pump power and the fluctuation of temperature of LBO. The red beam distribution is also shown in the inset of Fig. 10, and the average beam quality M^2 value was about 1.7, which was better than that of fundamental light, due to the fact that the nonlinear process during frequency

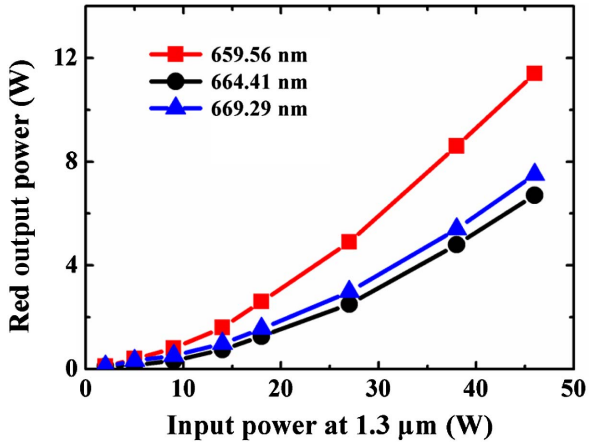

Fig. 9. Output power of the red laser as a function of the input power at 1.3 μm.

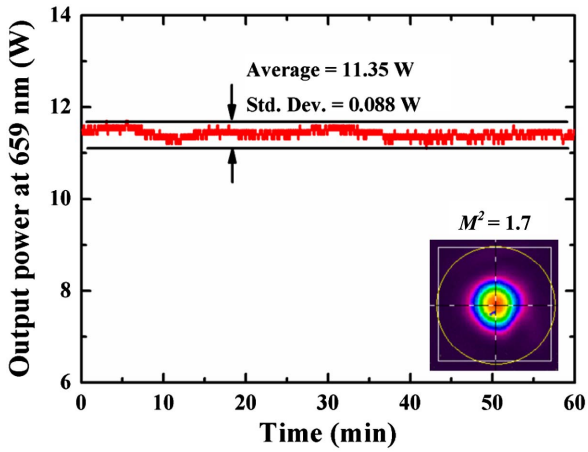

Fig. 10. Power stability test of red 659 nm laser over 1 h. Inset, 2D beam spatial profile.

doubling can filter out the stray light with low peak power. Besides, considering the practical application, one would be greatly concerned about the brightness B, which was proportional to laser power and inversely proportional to the square of the beam quality factor [2]. Accordingly, the maximal brightness of the frequency-doubled beam could be calculated to be 903 MW sr^{-1} cm^{-2}. Compared with the previously published works in Ref. [5] (6 W, $M^2 = 2.47$, $B = 218$ MW sr^{-1} cm^{-2}) and Ref. [19] (8.2 W, $M^2 = 1.65$, $B = 691$ MW sr^{-1} cm^{-2}), the present result is a significant improvement, especially for generating the ultraviolet 330 nm laser for the polychromatic laser guide star and the shortest deep-ultraviolet wavelength 165 nm laser for angle resolved photoemission spectroscopy.

4. CONCLUSION

In summary, high-power tunable single-wavelength and power-ratio-controllable dual-wavelength operations of a Q-switched Nd:YAG laser around 1.3 μm were demonstrated for the first time to our knowledge. The pulsed pumping technique was employed to improve the efficiency of the heat exchange in laser crystal. At a pump pulse duration of 200 μs with the repetition rate of 400 Hz, the laser for Q-switched operation delivered a pulse width of 117 ns with a beam quality of $M^2 = 1.87$. By introducing an etalon within the cavity, a single-wavelength Q-switched maximum output power is achieved to be 47.6 W at 1319 nm and 39.9 W at 1338 nm, whose linewidths are, respectively, 0.48 nm and 0.32 nm with a frequency stability of ±392 MHz and ±282 MHz. The simultaneous dual-wavelength oscillation with a balanceable and stable proportion delivered 45.7 W output power. Moreover, red light of 659 nm, 664 nm, and 659 nm was achieved by nonlinear frequency conversion of the laser. The experimental results prove to be a significantly improvement on 1.3 μm lasers to meet the versatile application.

Funding. National Natural Science Foundation of China (62005295); National Key Research and Development Program of China (2016YFB0402103).

Disclosures. The authors declare no conflicts of interest.

Data Availability. Data underlying the results presented in this paper are not publicly available at this time but may be obtained from the authors upon reasonable request.

REFERENCES

1. H. Liu, M. Gong, X. Wushouer, and S. Gao, "Compact corner-pumped Nd:YAG/YAG composite slab 1319 nm/1338 nm laser," Laser Phys. Lett. **7**, 124–129 (2010).
2. Q. Bian, J. W. Zuo, C. Guo, C. Xu, Y. Shen, N. Zong, Y. Bo, Q. J. Peng, H. B. Chen, D. F. Cui, and Z. Y. Xu, "Spiking suppression of high power QCW pulse 1319 nm Nd:YAG laser with different intracavity doublers," Laser Phys. **26**, 095005 (2016).
3. A. Saha, R. Debnath, D. S. Hada, and S. K. Beda, "Simultaneous oscillations of twelve wavelengths around 1.3 μm in quasi-CW Nd:YAG laser," Opt. Laser Technol. **94**, 112–118 (2017).
4. X. D. Mu and Y. J. Ding, "Efficient generation of coherent blue light at 440 nm by intracavity-frequency-tripling 1319 nm emission from a Nd:YAG laser," Opt. Lett. **30**, 1372–1374 (2005).
5. C. L. Du, S. C. Ruan, Y. Q. Yu, and F. Zeng, "6-W diode-end-pumped Nd:$GdVO_4$/LBO quasi-continuous-wave red laser at 671 nm," Opt. Express **13**, 2013–2018 (2005).
6. Y. F. Wan, K. Z. Han, Y. Wang, and J. L. He, "High power CW and *Q*-switched operation of a diode-side-pumped Nd:YAG 1319-nm laser," Chin. Opt. Lett. **6**, 124–126 (2008).
7. G. Zhang, H. Y. Zhu, C. H. Huang, J. Chen, Y. Wei, and L. X. Huang, "Diode-side-pumped Nd:YAG laser at 1338 nm," Opt. Lett. **34**, 1495–1497 (2009).
8. P. Li, X. H. Chen, H. N. Zhang, and Q. P. Wang, "Diode-end-pumped passively *Q*-switched 1319 nm Nd:YAG ceramic laser with a V^{3+}:YAG saturable absorber," Laser Phys. **21**, 1708–1711 (2011).
9. H. Aman, "1 mJ Passively *Q*-switched Nd:YAB laser using a V:YAG crystal," J. Russ. Laser Res. **34**, 59–62 (2013).
10. A. Saha, A. Ray, S. Mukhopadhyay, N. Sinha, P. K. Datta, and P. K. Dutta, "Simultaneous multi-wavelength oscillation of Nd laser around 1.3 μm: a potential source for coherent terahertz generation," Opt. Express **14**, 4721–4726 (2006).
11. Y. M. Duan, H. Y. Zhu, C. W. Xu, H. Yang, D. W. Luo, H. Lin, J. Zhang, and D. Y. Tang, "Comparison of the 1319 and 1338 nm dual-wavelength emission of neodymium-doped yttrium aluminum garnet ceramic and crystal lasers," Appl. Phys. Express **6**, 012701 (2013).
12. L. Guo, R. J. Lan, H. Liu, H. H. Yu, H. J. Zhang, J. Y. Wang, D. W. Hu, S. D. Zhuang, L. J. Chen, Y. G. Zhao, X. G. Xu, and Z. P. Wang, "1319 nm and 1338 nm dual-wavelength operation of LD end-pumped Nd:YAG ceramic laser," Opt. Express **18**, 9098–9106 (2010).
13. C. T. Wu, M. Yu, C. Wang, K. Yu, Y. J. Yu, X. Y. Chen, and G. Y. Jin, "LD end-pumped acousto-optic *Q*-switched 1319 nm/1338 nm dual-wavelength Nd:YAG laser," Opt. Commun. **376**, 26–29 (2016).
14. B. Lin, K. Xiao, Q. L. Zhang, D. X. Zhang, B. H. Feng, Q. N. Li, and J. L. He, "Dual-wavelength Nd:YAG laser operation at 1319 and 1338 nm by direct pumping at 885 nm," Appl. Opt. **55**, 1844–1848 (2016).
15. H. P. Cheng, Y. C. Liu, T. L. Huang, H. C. Liang, and Y. F. Chen, "Orthogonally polarized single-longitudinal-mode operation in a dual-wavelength monolithic Nd:YAG laser at 1319 nm and 1338 nm," Photon. Res. **6**, 815–820 (2018).
16. S. Singh, R. G. Smith, and L. G. Van Uitert, "Stimulated-emission cross section and fluorescent quantum efficiency of Nd^{3+} in yttrium aluminum garnet at room temperature," Phys. Rev. B **10**, 2566–2572 (1974).
17. W. Koechner, *Solid-State Laser Engineering*, 5th ed. (Springer, 1999).
18. C. Y. Li, Y. Bo, F. Yang, Z. C. Wang, Y. T. Xu, Y. B. Wang, H. W. Gao, Q. J. Peng, D. F. Cui, and Z. Y. Xu, "106.5 W high beam quality diode-side-pumped Nd:YAG laser at 1123 nm," Opt. Express **18**, 7923–7928 (2010).
19. P. F. Zhu, B. Li, W. Q. Liu, T. H. Liu, C. X. Fang, Y. Zhao, and Q. Zheng, "All-solid-state continuous-wave frequency doubling Nd:YAG/LBO Laser with 8.2 W output power at 660 nm," Opt. Spectrosc. **113**, 560–564 (2012).